THE JOURNAL OF PHYSICAL CHEMISTRY B

Article

pubs.acs.org/JPCB

Effect of the Degree of Dissociation of Molecules in a Monolayer at an Air/Water Interface on the Force Between the Monolayer and a Like-Charged Particle in the Subphase

Cathy E. McNamee,*[,†] Michael Kappl,[‡] Hans-Juergen Butt,[‡] Hang Nguyen,[†] Shinichiro Sato,[†] Karlheinz Graf,[§] and Thomas W. Healy[∥]

[†]Shinshu University, Ueda, 386-8567, Japan

[‡]Max Planck Institute for Polymer Research, Mainz, 55128, Germany

[§]Physical Chemistry, University of Applied Sciences, Krefeld, 47798, Germany

[∥]Particulate Fluids Processing Centre, The University of Melbourne, Melbourne, 3010, Australia

ABSTRACT: We used the monolayer particle interaction apparatus to measure the force between a monolayer of stearic acid or octadecanol at the air/water interface and a colloidal silica sphere. The silica sphere approached the monolayer from the aqueous subphase. The aim was to analyze how the magnitude of the charge of a deformable interface affects the interaction between that interface and a like-charged hard particle. The charge density of the stearic acid monolayer was controlled by adjusting the pH (5.8−9) and the surface pressure. The octadecanol monolayer acted as a reference; the alcohol headgroup did not dissociate between pH 5.8−9.0. Stable monolayers of dissociated stearic acid molecules were formed at the air/water interface by dissolving stearic acid into the subphase to give a saturated concentration at each pH value studied. The approach force curve showed that the electrostatic repulsion increased with an increasing degree of dissociation and therefore the charge of the monolayer. The strength of the repulsion corresponded to that measured between two like-charged hard surfaces, but the apparent range of the repulsion was larger for a deformable interface. Retracting force curves displayed a significant adhesion, whose magnitude and range depended on the surface pressure and subphase pH.

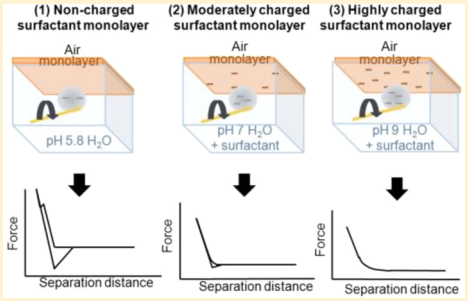

1. INTRODUCTION

Control over the interaction between deformable interfaces and particles is vital in many nano- and biotechnological applications, such as the stability of emulsions against coalescence and foam stability in food technology,[1] the interaction between catheters and the deformable cystic duct in medical applications,[2] flotation,[3] and the deinking of paper.[4,5]

The physical interactions between two hard interfaces in an aqueous solution can be controlled by the charge density or the surface potential and the concentration of ions in the solution. In the case of the interaction between a fluid interface and a hard surface, the viscosity will also affect the interactions. In addition, a hard particle interacting with a liquid/gas interface may penetrate the interface and form a three-phase contact line. The effect of the charge of the surface on the forces between a deformable interface and a hard surface is not well-known.

Interactions between deformable surfaces and a hard particle have been indirectly studied via methods such as contact angle[6,7] and interfacial tension measurements.[8−10] Direct force measurements have been carried out using atomic force microscopy[11−17] and the surface force apparatus[18] for interactions between a hard particle or substrate and an oil droplet[11,12,14] or an air bubble[15] in aqueous solutions. A decane/aqueous interface in the presence of an anionic surfactant was seen by an atomic force microscope to give repulsive forces, whose range and magnitude decreased with an increased surfactant concentration.[19] Such a repulsive force can be explained by an electrostatic double-layer force arising from the charge of the oil/water interface. The presence of interfacial charges was verified by zeta potential measurements of various oil drops in an aqueous phase containing NaCl in the absence of surfactants,[20,21] and/or the charge resulting from the adsorption of the surfactants to the oil/water interface. The charge of a deformable interface is expected to affect the forces measured between a deformable interface and a hard particle. However, the way the magnitude of the charge affects the interface−particle interaction and therefore the physical properties of the system is not clearly understood.

Forces between a particle and a charged monolayer at the air/water interface can be measured by using the monolayer particle interaction apparatus (MPIA). We recently studied the effect of the sign of the charges between fully charged monolayers at air/aqueous interfaces and charged particles in the subphase.[22] Repulsive forces dominate in the approach force curves at all separations for similarly charged systems. Attractive forces are present at smaller separations for

Received: July 25, 2012
Revised: September 28, 2012
Published: October 23, 2012

oppositely charged systems.[22] Here, we aim to study how the magnitude of the charge in a monolayer at the water/air interface affects the forces on a like-charged particle approaching the monolayer from the subphase aqueous solution. This was achieved by using the MPIA to study the forces between monolayers of different charge densities at air/water interfaces and a negatively charged silica particle in the subphase. The monolayer was formed from stearic acid, and the degree of dissociation was varied by changing the pH of the subphase. The charge of the monolayer was controlled via the degree of dissociation of the stearic acid and the surface pressure of the monolayer. For comparison, the interaction between a particle and a monolayer of octadecanol was measured. The alcohol headgroup of the octadecanol does not dissociate over the pH range 5.8−9.0.

2. EXPERIMENTAL SECTION

2.1. Materials. The materials used in this experiment were octadecanol (99.5% purity, Fluka, Germany), stearic acid (99% purity, Fluka, Germany), chloroform ($CHCl_3$, >99% purity, ACROS Organics, Belgium), ethanol (EtOH, >99.5% purity, Sigma-Aldrich, Germany), and sodium chloride (NaCl, 99.8% purity, WTL Laborbedarf GmbH, Kastellaun, Germany). The water used in this study was distilled and deionized using a water purification system (Direct-Q3 UV, Millipore, USA, or a Satorius water purification system, 18.2 MΩcm). The pH of the solutions was adjusted by using sodium hydroxide (NaOH, 97% purity, Wako, Japan) and tested with a pH meter (compact pH meter twin, Horiba, Japan).

Aqueous solutions saturated with stearic acid were prepared by first adding stearic acid to the water solution of the required pH. The stearic acid was dissolved to saturation by hand-mixing the solution, sonificating for 1 h, and then by leaving the solution overnight. The solution was then filtered using filter paper (Whatman 101, Japan), in order to remove any undissolved stearic acid. The filtered solution was used as the subphase in the monolayer studies.

The silica particles (nominal diameter (D) = 6.84 μm, Bangs Laboratory, Fishers, USA) were attached by using a micromanipulator (Model MMO-203, Narishige, Tokyo, Japan) and a light microscope (Zeiss, Axiotech vario 100 HD) to a gold-plated Si_3N_4 cantilever (V-shape, 200 μm long, nominal spring constant k = 0.15 N/m, OMCL-TR800PSA, Olympus, Japan) with epoxy resin (Araldite Rapid, Nichiban, Japan). The silica probe was cleaned immediately before each MPIA experiment by plasma treatment (PDC-002, Harrick Plasma, Ithaka, USA) under argon gas for 1 min.

2.2. Methods. *2.2.1. Preparation of Langmuir Monolayers and Measurement of Surface Pressure−Area per Molecule Langmuir Isotherms.* The monolayers in this study were prepared using a poly(tetrafluoroethylene) (PTFE)-coated Langmuir trough (Riegler & Kirstein GmbH, Potsdam, Germany) equipped with two PTFE barriers that compressed around the center of the trough (compression ratio 1:11, max. area between the barriers: 349 cm^2). The temperature of the subphase was kept at 20.0 ± 0.1 °C by using a circulation system (C25P, ThermoHaake, Karlsruhe, Germany) to run thermostatted water through the metal base of the trough. The surface pressure of the monolayer was measured using a Wilhelmy plate, where wetted filter paper[23] (S&S 595 Filter Paper Circles, Schleicher & Schuell GmbH, Dassel, Germany) was suspended from a strain gauge (Riegler & Kirstein GmbH, Potsdam, Germany).

The surface pressure (Π)−area per molecule (A) isotherms were measured by cleaning the Langmuir trough with chloroform and with ethanol, after which water was added and its surface cleaned by compressing the barriers to maximum, aspirating the surface between the barriers, and then expanding the barriers. The surface pressure−area isotherm that gave Π = 0 ± 0.5 mN/m at all A showed that the water surface was clean. The octadecanol or stearic acid monolayer was subsequently prepared by spreading 40 μL of a 3.12 mM solution of octadecanol in $CHCl_3$ or 3.23 mM solution of stearic acid in $CHCl_3$ dropwise at the air/water interface using a 50 μL syringe (705RN, Hamilton, Switzerland). After waiting 10 min to allow for the evaporation of the $CHCl_3$, the barriers were compressed at a speed of 3.13 cm^2 s^{-1}, which corresponds to a speed of 0.42 and 0.39 $Å^2 molecule^{-1}$ s^{-1} for octadecanol and stearic acid, respectively. The surface pressure and area per molecule were measured simultaneously in order to generate the Π−A isotherms.

2.2.2. Monolayer Particle Interaction Apparatus and Measurement of Force Curves. The simultaneous measurement of the interaction between a colloid probe and a monolayer at the air/liquid interface and the Π−A isotherm of the monolayer was achieved using the MPIA (Figure 1). It is composed of the Langmuir trough described above and a force measurement unit. Briefly, the colloid probe was secured using a cantilever holder (PEEK, MPIP, Mainz, Germany), inserted from above through the small hole that was in the exchangeable glass window in the base of the film balance, and connected to a closed loop piezo translation stage (model P-753.21C, 25 μm range, PI, Karlsruhe, Germany). Leakage of water from the trough was avoided by sealing the cantilever holder and the glass window hole area with an O-ring (Viton-Seal 5 × 9 × 2, DFV-Dichtungen, Berlin, Germany). The distance between the probe and monolayer was varied by applying a voltage to a digital piezo controller (model E-661.CP), which caused the cantilever holder to move up or down in the z-direction. The forces acting between the colloid probe and the monolayer in the liquid subphase were measured by optically detecting the

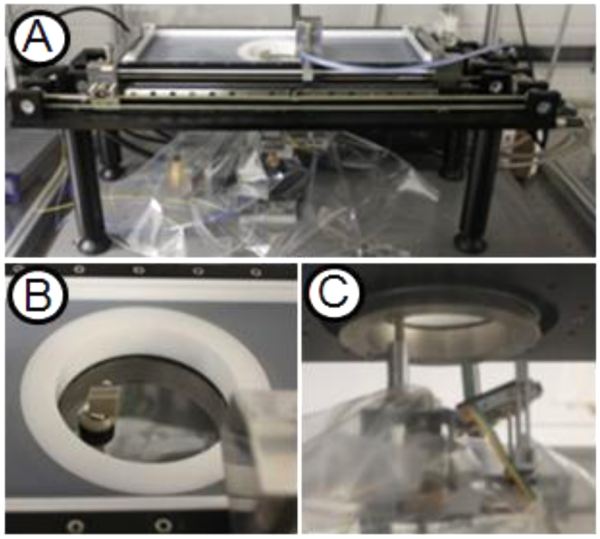

Figure 1. Photo of the MPIA used to measure the force curves in this study. (A) The MPIA as seen from the side; (B) the cantilever holder, O-ring, and glass plate as seen from above; (C) the piezo, photodetector, and glass plate as seen from below.

change in the deflection of the cantilever (Δx) as a function of the piezo position by reflecting a laser beam (λ = 658 nm, $P_{out} \leq$ 5 mV, FKP-620−23, Schäfter + Kirchhoff, Hamburg, Germany) from the underside of the cantilever onto a highly linear position sensing detector (PSD, L2L20SP, Laser Components, Olching, Germany). The detection of the laser beam from the probe through the trough and then back to the PSD was possible due to the exchangeable glass window in the base of the film balance. The change in the deflection, i.e., Δx, was detected by a change in the position of the laser reflected onto the PSD. The Δx was converted from volts to nanometers by using the constant compliance region of a force curve that was measured between the same colloid probe and a hard substrate (the underside of a mica plate glued to a glass substrate that was placed across the top sides of the Langmuir trough). The position of zero separation for the particle−hard substrate system was defined as the position of the onset of the linear compliance region in the force profile. The position of zero distance in the force−distance curves of the particle−monolayer system was defined as the onset of the linear repulsion region, which occurred after the probe was in contact with the monolayer at the air/liquid interface (the "contact regime"). Hooke's law, $F = k\Delta x$, was used to calculate the force (F) between the probe and the interface, where k is the spring constant of the cantilever. Zero force was defined to occur at large cantilever−substrate separations, a position where no surface forces act on the cantilever.

The forces were measured using the MPIA by first attaching the colloid probe to the cantilever holder, which was then inserted through the hole in the base of the Langmuir trough and attached to the piezo. Water was added to the trough, and the water surface was cleaned by suctioning in the manner described above. The forces between the probe and a clean mica substrate that was placed across the edges of the Langmuir trough were then measured in the water, in order to obtain the volt-to-nanometer calibration factor for the probe−monolayer force curves. The water surface was then suction cleaned again, and the forces were measured using the same probe against a clean air/water interface in the absence of a monolayer. The water was then removed, the solution to be used as the subphase in the monolayer force measurements was added to the trough, and the subphase surface was cleaned by compression and suctioning. A monolayer of octadecanol or stearic acid was spread on the subphase surface. The monolayer was subsequently compressed to the desired surface pressure, which was maintained constant by enabling the constant surface pressure feedback control of the Langmuir trough. The forces were measured between the probe and the underside of the monolayer by recording Δx as the probe was moved from the bulk solution to the underside of the monolayer. The load (F_L) applied was controlled so that the adhesion forces were not affected by F_L. This was important as we previously found that different values of adhesion forces may be obtained if high values of F_L were used.[24] The forces were measured in the order of low to high surface pressure, and a minimum of 100 force curves were measured for each surface pressure. The average adhesion force (F_{ad}) between the probe and the monolayer was determined by fitting a Gaussian curve to a histogram of the adhesive forces measured at a given Π. The reduced F_{ad} data term of F_{ad}/R^2 was used instead of F_{ad} to compare the F_{ad} of different systems, where R is the particle radius. This was because we previously found that the size of the particle used in the measurement of forces of deformable interfaces is only irrelevant if F_{ad} is scaled by R.[2,24] Such a scaling will also enable the future comparison of this adhesion data with other systems. The effective stiffness (S_N)[24] of the air/monolayer/aqueous interface was calculated by dividing the slope of the linear contact region in the force curve recorded between a colloid probe and a monolayer at the air/aqueous interface (S_1) by the slope of the linear contact region in the force curve recorded between the same colloid probe and a mica substrate (S_2) in water.

3. RESULTS AND DISCUSSION

3.1. Surface Pressure versus Area Per Molecule Isotherms. Monolayers of stearic acid and of octadecanol were formed on pH 5.8, pH 7, and pH 9 water surfaces. Their surface pressure versus area per molecule isotherms are shown in Figure 2. At pH 5.8 the stearic acid and octadecanol

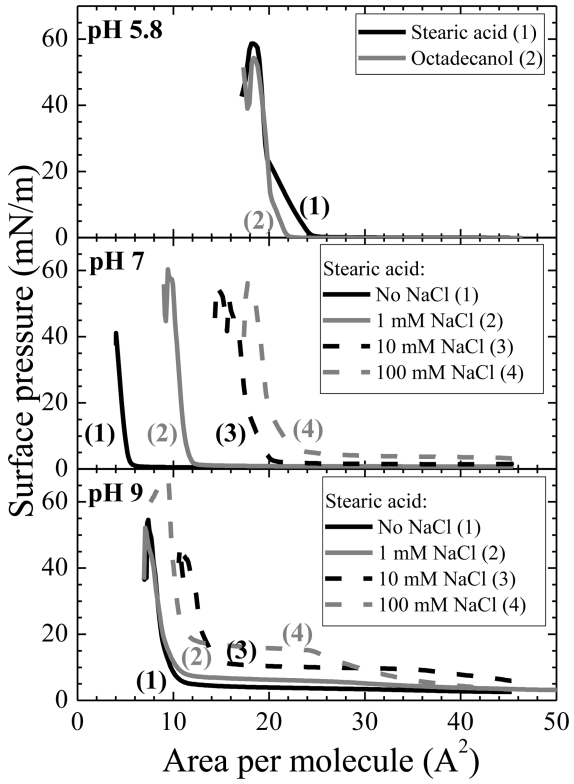

Figure 2. Surface pressure−area per molecule isotherms for octadecanol and stearic acid monolayers at air/aqueous interfaces at different pH and salt concentrations recorded 10 min after spreading.

isotherms were similar in shape and position. Both monolayers displayed a gaseous, a liquid-expanded, and a solid regime. The limiting area per molecule of both monolayers was 20 Å^2, in agreement with previous studies.[25,26] At pH 5.8, the addition of 100 mM NaCl to the subphase did not affect the Π−A isotherms of the stearic acid or octadecanol monolayers. This indicates that these monolayers were sufficiently cohesive to avoid any squeezing out of molecules into the subphase.

Changing the pH of the subphase to 7.0 and the subsequent addition of NaCl did not affect the Π−A isotherms of the octadecanol monolayer. However, the isotherm of the stearic acid monolayer shifted to a lower limiting area per molecule (A_0) for a pH 7.0 subphase. The addition of salt shifted the stearic acid isotherm to the right, i.e., larger values of A_0. A subphase with 100 mM NaCl gave an isotherm with a limiting

dx.doi.org/10.1021/jp307343a | J. Phys. Chem. B 2012, 116, 13731−13738

area of approximately 20 Å^2 that was in agreement with that measured at pH 5.8. The reduced area per molecule at pH 7.0 indicates that the stearic acid is moving from the interface into the bulk phase, due to the increased solubility of the carboxylic acid anion at pH values well above the pK_a. The plateau region of ca. 25−12 Å^2 that follows the gaseous region of the Π−*A* curves for stearic acid at pH 7.0 for 10 and 100 mM NaCl is probably a region where squeezing out of the molecules into the subphase occurs. It is followed by a pseudo-solid phase compression being displayed by the molecules remaining in the monolayer.

Increasing the pH to pH 9.0 and the subsequent addition of salt did not affect the Π−*A* isotherms of the octadecanol monolayer. This indicates that octadecanol does not dissociate between pH 5.8 and pH 9.0. This result indicates that the stearic acid is highly dissociated at pH 9.0, and does not form a stable, insoluble monolayer at the air/water interface. A similar result showing a shift in the Π−*A* isotherms of a stearic acid monolayer to lower *A* with a pH increase from 4.0 to 10.0 has been reported by Avila and others[27] and Goddard and Ackilli.[26]

Stearic acid has a pK_a of 5.0.[28,29] The solubility of stearic acid increases from 10^{-8} M at pH 5.8 to 3.7×10^{-7} M at pH 7, and to 10^{-5} M at pH 9.[28,30] This solubility increase would promote the squeezing out of stearic acid from the air/water interface to the bulk water. It is also known that stearic acid monolayers at very high pH can be stabilized by the addition of counterions in the subphase.[31−33] If the subphase contains a saturated concentration of stearic acid, then there should not be any further transport of molecules from the stearic acid monolayer into the bulk phase. Figure 3 shows that the addition of stearic

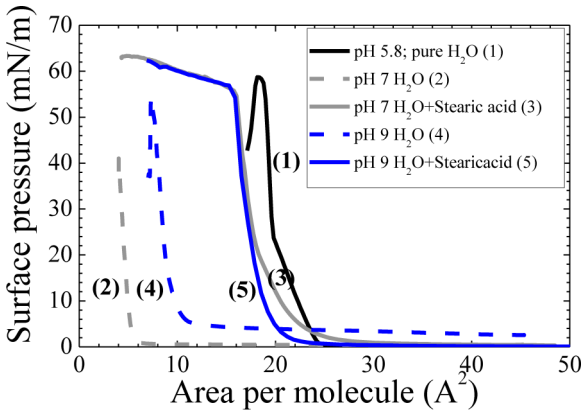

Figure 3. Surface pressure−area per molecule isotherms of the stearic acid monolayer at air/aqueous interfaces with and without stearic acid in the subphase at pH 5.8, pH 7, and pH 9.

acid to the subphase to the solubility limit for the pH 7.0 and pH 9.0 systems shifts the Π−*A* isotherms from lower to higher area per molecules toward the expected limiting area of 20 Å^2. The stearic acid monolayer at the interface was stable, and the Π−*A* isotherms were not affected by the compression speed or the time elapsed after spreading the monolayer and before compression of the monolayer. These results indicate that the number of stearic acid molecules in the monolayer did not change. Thus, the dissolution of the stearic acid molecules from the monolayer into the subphase is avoided. The limiting areas per molecule of the isotherms at the pH 5.8, pH 7.0 + stearic acid, and pH 9.0 + stearic acid subphases are 20.0, 19.3, and 15.0 Å^2, respectively (Figure 3). The decrease from 20 to 15 Å^2 probably reflects the fact that the subphases at high pH were not fully saturated. These limiting areas are similar to those obtained for a stearic acid monolayer at pH 9.1 and pH 11.1 subphases containing salt, which were between 20.2 and 18.6 Å^2.[31−33] Thus, a stable monolayer of dissociated stearic acid can be formed at an air/water interface without the need of adding salts, if stearic acid is dissolved in the subphase to give the concentration of the solubility limit.

3.2. Force Curves. Increasing the pH of the subphase increases the charge of the stearic acid monolayer. In order to interpret and understand the influence of the charge on the forces, we compared the forces measured in the subphase with a silica probe against air/water interfaces of pH 5.8, 7.0, and 9.0 and against air/water + stearic acid interfaces of pH 7.0 and 9.0, in the absence of Langmuir monolayers (Figure 4). Forces

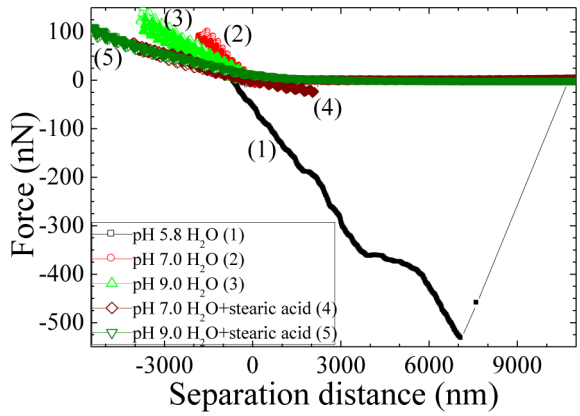

Figure 4. Force curves for the air/water interface in the absence of a Langmuir monolayer when the pH of the water subphase was varied and stearic acid was added to the bulk water. The open and solid symbols show the approach and retract force curves, respectively.

measured at air/water interfaces without stearic acid showed a steep, linear repulsive force, assigned as the contact regime. Addition of stearic acid to the subphase caused the slope of the contact regime to decrease. In other words: the stiffness of the interface decreased. Increasing the subphase pH from 5.8 to 9.0 increases the solubility of stearic acid, resulting in an increase in the concentration of stearic acid in the subphase. The addition of stearic acid to the subphase of pH 9.0 caused a nonlinear repulsive force to be observed before the steep, linear repulsive force of the contact regime. Addition of ions (Na^+, OH^-) or stearic acid to the subphase also caused the magnitude and extent of the adhesion to decrease. The increase in the nonlinear repulsion and the decrease in adhesion with pH and the addition of stearic acid to the subphase is attributed to an electrostatic double-layer repulsion between the negatively charged silica particle and the interface. The interface is strongly negatively charged at pH 9, due to the dissociated stearic acid molecules.

Force curves obtained from repetitive measurements for a stearic acid monolayer and an octadecanol monolayer at a low (10 mN/m) and a high (40 mN/m) surface pressure are shown in Figure 5. No salt was added for the octadecanol systems or the pH 5.8 stearic acid system. The forces for the stearic acid monolayers were measured on a subphase saturated with stearic acid in the case of pH 7.0 and pH 9.0. Comparison of the force curves measured against a bare water surface (Figure 4) and against a monolayer covered surface (Figure 5) showed a

dx.doi.org/10.1021/jp307343a | J. Phys. Chem. B 2012, 116, 13731−13738

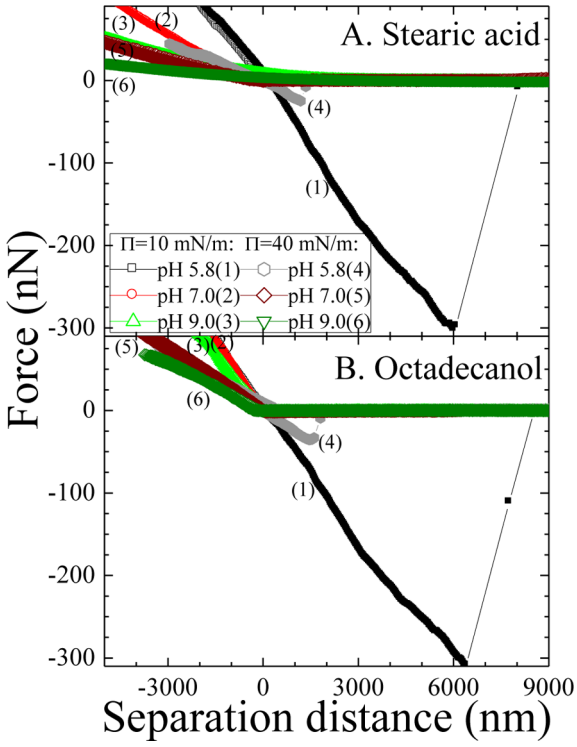

Figure 5. Force curves obtained from repetitive measurements for the (A) stearic acid Langmuir monolayer and (B) octadecanol Langmuir monolayer at a low (10 mN/m) and a high (40 mN/m) surface pressure. The open and solid symbols show the approach and retract force curves, respectively.

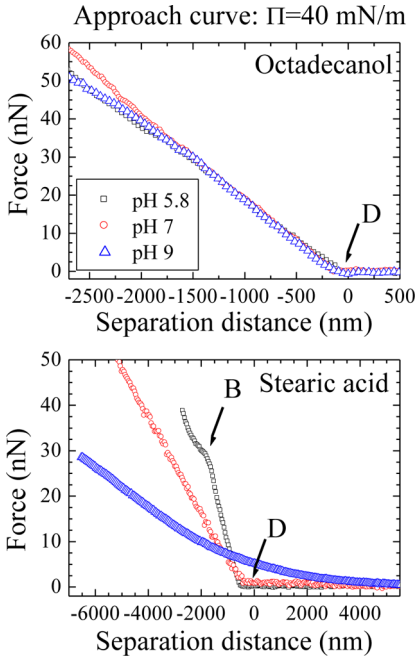

Figure 6. Expanded force curves from Figure 5 showing the approach force curves of the octadecanol and stearic acid monolayers at a compressed packing of 40 mN/m on pH 5.8, pH 7, and pH 9 subphases. The subphase for the stearic acid monolayer at pH 7 and pH 9 contains stearic acid. The arrows indicate the onset of deformation (D) and the position of break-through (B), where the particle forms a three-phase contact region with the air, monolayer, and subphase.

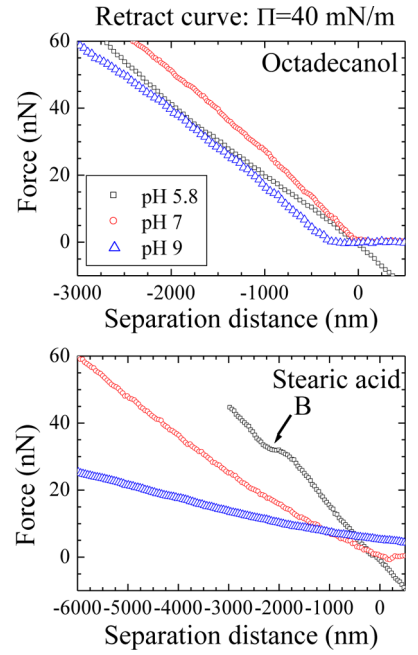

Figure 7. Expanded force curves from Figure 5 showing the retract force curves of the octadecanol and stearic acid monolayers at a compressed packing of 40 mN/m on pH 5.8, pH 7, and pH 9 subphases. The subphase for the stearic acid monolayer at pH 7 and pH 9 contains stearic acid. The arrows on the graph indicate the position of break-through (B).

decrease in the fluctuations (oscillations) apparent in the force curves. On bare water, the vibrations of the water surface usually lead to significant fluctuations in force curves. This was reduced when surfactant was added, indicating that vibrations are significantly damped in the presence of surfactants. The approach curves of the monolayer systems all displayed a linear repulsive force. The onset of this repulsion ("D" on Figure 6) was followed by deformation repulsion and then a discontinuity at high force, which is evidence of a break-through ("B" on Figure 6). In the case of a stearic acid monolayer, the deformation on the approach force curve was followed by a break-through at a force of ~30 nN for a pH 5.8 subphase, respectively. No break-through was observed at pH 7.0 or pH 9.0. Additionally, the approach force curves at pH 9.0 appeared different from those measured at pH 5.8 and pH 7. A long-range nonlinear repulsive force was observed before the onset of the nonlinear region in the case of a stearic acid monolayer. The slope of this linear repulsion decreased with increasing surface pressure and pH for the stearic acid and octadecanol monolayers. The retract force curve showed a repulsive part and an adhesion, after which the particle and the monolayer separated. A discontinuity was also observed on the repulsive part of the retract force curve (B in Figure 7). The magnitude and range of the adhesion decreased with an increase in pH or surface pressure.

The ratio of dissociated/undissociated carboxyl groups in the stearic acid monolayer increases from 50%/50%, 90%/10%, and to 99%/1% as the pH increases from 5.8, 6.8, and to 7.8.[34] Thus, at pH 9 the stearic acid monolayer is essentially fully charged. Therefore, the repulsion between the monolayer and the particle is large. The repulsive force occurring before the deformation regime is interpreted as an electrostatic double-layer repulsion between the negatively charged monolayer and

dx.doi.org/10.1021/jp307343a | J. Phys. Chem. B 2012, 116, 13731−13738

the negatively charged silica particle. The octadecanol monolayers gave no such long-range repulsion, although the zeta potential of the octadecanol monolayer at an air/water interface has been measured to increase from −70 to −82 mV for a pH increase from 5.8 to 9.[35] The negative zeta potential of the octadecanol monolayer has been explained by Usui and Healy[35] as being due to the dissociation of protons from the water molecules that hydrate the OH groups of the monolayer surface. This suggests that the dissociated protons do not affect the force curves in a manner that can be detected by the MPIA.

In order to determine whether the repulsive force can be explained by an electrostatic interaction, we calculated the electrostatic free energy of interaction per unit area (E_{DL}) between two planar parallel non-deformable surfaces at a given separation x by using[36]

$$E_{DL}(x) = \frac{\varepsilon_0 \varepsilon_r \kappa}{2}[2\Psi_{01}\Psi_{02}\ \mathrm{cosech}\ \kappa x - (\Psi_{01}^2 + \Psi_{02}^2)(1 - \coth \kappa x)] \quad (1)$$

Here, ε_r, ε_0, $1/\kappa$, Ψ_{01}, andΨ_{02} are the relative permittivity of the electrolyte solution, the permittivity of vacuum, the Debye length, the surface potential of one surface, and the surface potential of the other surface, respectively. Equation 1 was derived assuming a constant surface charge density.[36] The surface potentials of the stearic acid, octadecanol, and silica surfaces were estimated using the zeta potential values of an insoluble monolayer of a carboxylic acid (RCOOH) and octadecanol at an air/water interface,[37] an insoluble monolayer of an alcohol (ROH) at an air/water interface,[35] and a hard silica surface[38] in a 1 mM salt solution of pH 5.8, pH 7, and pH 9 (Table 1). Figure 8 shows that the magnitude of E_{DL} increases

Table 1. Zeta Potentials of Stearic Acid Monolayer (RCOOH), an Octadecanol Monolayer (ROH), and Silica in 1 mM NH_4NO_3 Solution[35,37,38]

	zeta potential (mV)		
pH	RCOOH	ROH	silica
5.8	−120	−70	−58
7	−135	−75	−88
9	−150	−82	−100

with a pH increase for both the stearic acid and octadecanol cases. As the unadjusted pH of our pure water was 5.8, the number of OH^- ions in our water increased as the pH was increased from 5.8 to 9 due to the addition of NaOH. Thus, an increase in the pH decreased the range of the electrostatic forces, in accordance with the increased concentration of OH^- and Na^+ ions. Forces measured for the stearic acid are stronger than for octadecanol, due to the higher surface potential of the stearic acid. These trends are consistent with the measured force curves. The range of electrostatic repulsion between the deformable interface and the silica particle is stronger than that predicted by the above model for the interaction between two hard surfaces. Given that the water surface and the monolayer are deformable, the distance of the overlaps of the electrostatic repulsions resulting between a deformable and a hard surface is expected to be greater than that between two hard surfaces.

The retract force curves measured for a bare air/water interface, a stearic acid monolayer or an octadecanol monolayer at an air/water interface displayed an adhesive force with a single adhesion maximum. The magnitude and extent of the

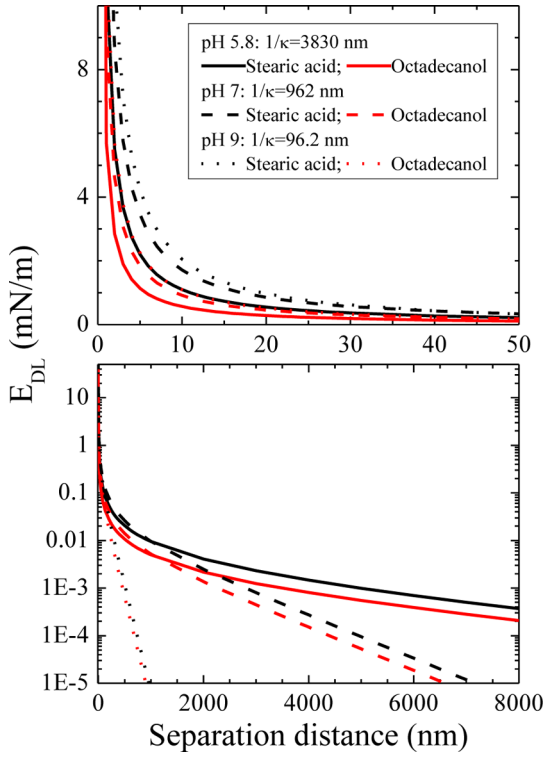

Figure 8. Electrostatic interaction (E_{DL}) versus separation distance between a silica hard surface and a stearic acid or octadecanol hard surface calculated by using the solution for a constant charge density of a dissimilar system.

adhesion maximum depended on the pH, the interface type, and the surface pressure. Generally, a pH increase decreased the adhesion maximum. The contact angle of silicon for water has been reported to decrease from around 38° to 27° as the pH is increased from pH 5 to pH 10.[39] Since adhesion due to the capillary force and contact angle (θ) are related by[40,41]

$$F = 2\pi\gamma R\ \cos^2(\theta/2) \quad (2,)$$

this decrease in adhesion with a increasing pH is explained by the improved wetting conditions. An increased adhesion between a particle and a bubble in solution has been reported to increase with increased contact angle.[42] As an electrostatic or steric repulsion has been reported to cause a stable wetting film on a substrate,[43] an electrostatic double-layer repulsion between the monolayer and the silica particle may cause this improved wetting with a pH increase. A discontinuity was measured at high forces after deformation on the approach curves for the cases where an adhesive force was also measured in the retract force curves. This discontinuity is therefore thought to be the result of the onset of the formation of a three-phase contact regime, i.e., the top of the silica particle is in contact with the air, monolayer, and subphase. The discontinuity that was observed on the repulsive portion of the retract force curve is thought to be where the probe re-enters the subphase.

The effect of the surface pressure, monolayer types, and pH on the force curves between the monolayers at the air/water interface and a silica particle can be easier seen by determining the reduced adhesion maximum (F_{ad}/R^2) and the stiffness (S_N) of the monolayer from the experimental force curves (Figure 9). The reduced adhesion decreased with a pH increase for both stearic acid and octadecanol monolayers. This can be

dx.doi.org/10.1021/jp307343a | J. Phys. Chem. B 2012, 116, 13731−13738

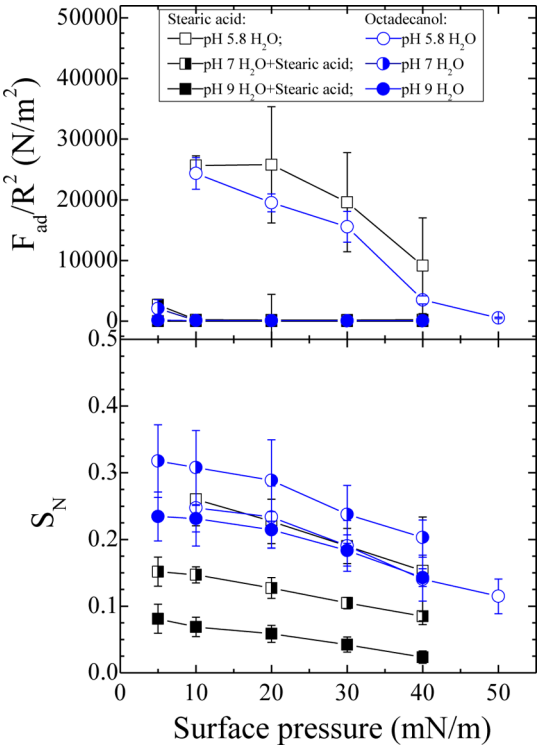

Figure 9. Dependence of the reduced adhesion, F_{ad}/R^2, and S_N on the surface pressure of the monolayer and the monolayer type and subphase pH, obtained from the force curves measured between a bare silica probe and a stearic acid or octadecanol monolayer at an air/aqueous interface. The black and blue symbols refer to the stearic acid and octadecanol monolayer data, respectively. The open, half solid, and solid symbols are for the pH 5.8, pH 7, and pH 9 water subphases, respectively.

explained by the increased wetting of a silica surface by higher pH solutions. Additionally, the surface potential of an air/water interface increases from −110, −130, to −155 mV with a pH increase from 5.8, 7, to 9.[44] Thus, there is an increased electrostatic repulsion between the silica particle and the air/water interface, which would also reduce the adhesion.

The stiffness decreased with pH for the stearic acid monolayer, but did not significantly change for the octadecanol monolayer. An increase in pH required stearic acid to be added to the subphase to achieve a stable monolayer. Some of those stearic acid molecules adsorb to the air/water interface, thereby reducing the surface tension. This would result in decreasing the stiffness of the interface. The octadecanol monolayer was stable, i.e., did not show squeezing out effects, at air/water interfaces and therefore did not require the addition of octadecanol in the subphase for higher pH measurements. The constant stiffness for octadecanol reflects the fact that the low charge electrical double layer at the alcohol−water interface[35] has little effect on the force curves.

An increase in the surface pressure due to compression of the stearic acid and octadecanol monolayers decreased both the reduced adhesion as shown in retraction curves and the stiffness, as shown in the approach curves. An increased surface pressure (decreased surface tension) leads to an increased electrostatic repulsion and a decreased stiffness of the interface. The former is due to the charge density of the monolayer increasing with increasing surface pressures, caused by the denser packing of the surfactants. The latter is due to the decreased interfacial stiffness caused by the decreased surface tension that is associated with an increased surface pressure. This makes the interface more deformable, which is reflected by a decreased slope in the contact regime of the force curves.[24] Figure 10 shows the linear relationship between the decrease in

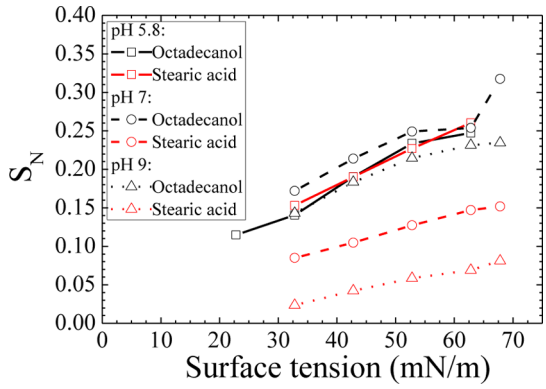

Figure 10. Variation of the stiffness of the monolayers as a function of the surface tension of the interface.

the stiffness measured with a decreased surface tension. The stearic acid Π−*A* curves on stearic acid saturated substrates, and the octadecanol pressure area curves all show the normal gaseous to liquid condensed to solid Π−*A* characteristics. Thus, a larger adhesion at low surface pressures can be concluded to be due to break-through. The lower adhesion observed at higher surface pressures is due to the increased electrostatic repulsions between the negatively charged monolayer and the negatively charged silica particle. Again, high surface pressure and the resulting high packing density of the surfactants results in a decrease in the surface tension and the stiffness of the interface. Information on the interaction between the molecules in the monolayer at the air/water interface and the particle in the subphase can therefore be obtained at high surface pressure regions, where the molecules are densely packed.

4. CONCLUSIONS

An increase in the dissociation of stearic acid molecules decreases their adsorption strength at an air/water interface. Saturated concentrations of stearic acid in the subphase allowed the formation of stable monolayers of dissociated molecules at the air/water interface. Force curves recorded between the air/water interface and a silica particle in the aqueous phase showed that decreasing the surface tension (either by increasing the surface pressure or by increasing the concentration of dissolved stearic acid) leads to a decreasing stiffness of the monolayer. Increasing the charge of a monolayer increased the electrostatic repulsion between monolayer and particle. The change in the magnitude of the repulsion corresponds to that measured in the force curves between two like-charged hard surfaces. However, the range of the repulsions is larger for the deformable case than the nondeformable case. The correlation between the discontinuity observed in the approach force curves at high forces, i.e., a break-through, and an adhesion force in the retract force curve indicates a three-phase contact formation of the particle with the air/subphase interface. The magnitude of the maximum in a retract force curve gives information on the break-through or wetting ability of the particle by the air/water interface.

dx.doi.org/10.1021/jp307343a | J. Phys. Chem. B 2012, 116, 13731−13738

AUTHOR INFORMATION

Corresponding Author

*E-mail: mcnamee@shinshu-u.ac.jp; Tel.: +81-(0)268-21-5585.

Notes

The authors declare no competing financial interest.

ACKNOWLEDGMENTS

The authors would like to thank Prof. Ko Higashitani (Kyoto University, Japan) and Prof. Derek Chan (The University of Melbourne, Australia) for valuable discussions. This study was performed through the Program for Dissemination of Tenure-Track System funded by the Ministry of Education and Science, Japan. H.J.B. acknowledges financial support of the DFG (Bu 1556/27).

REFERENCES

(1) Dickinson, E. *J. Chem. Soc., Faraday Trans.* **1992**, *88*, 2973−2983.
(2) Basdogan, C.; Ho, C. H.; Srinivasan, M. A. *IEEE-ASME Trans. Mechatronics* **2001**, *6*, 269−285.
(3) Ralston, J.; Dukhin, S. S.; Mishchuk, N. A. *Adv. Colloid Interface Sci.* **2002**, *95*, 145−236.
(4) Aston, D. E.; Berg, J. C. *J. Pulp Pap. Sci.* **1998**, *24*, 121−125.
(5) Vashisth, C.; Bennington, C. P. J.; Grace, J. R.; Kerekes, R. J. *Resour. Conserv. Recycl.* **2011**, *55*, 1154−1177.
(6) Karis, T. E.; Nayak, U. V. *Tribol. Trans.* **2004**, *47*, 103−110.
(7) Lucassen, J. *Colloids Surf.* **1992**, *65*, 139−149.
(8) Babak, V. G. *Usp. Khim.* **1993**, *62*, 747−773.
(9) Leonforte, F.; Servantie, J.; Pastorino, C.; Muller, M. *J. Phys.: Condens. Matter* **2011**, *23*, 184105.
(10) Hartley, P. G.; Grieser, F.; Mulvaney, P.; Stevens, G. W. *Langmuir* **1999**, *15*, 7282−7289.
(11) Nespolo, S. A.; Chan, D. Y. C.; Grieser, F.; Hartley, P. G.; Stevens, G. W. *Langmuir* **2003**, *19*, 2124−2133.
(12) Chan, D. Y. C.; Dagastine, R. R.; White, L.R. J. *Colloid Interface Sci.* **2001**, *236*, 141−154.
(13) Aston, D. E.; Berg, J. C. *J. Colloid Interface Sci.* **2001**, *235*, 162−169.
(14) Mulvaney, P.; Perera, J. M.; Biggs, S.; Grieser, F.; Stevens, G. W. *J. Colloid Interface Sci.* **1996**, *183*, 614−616.
(15) Butt, H.-J. J. *J. Colloid Interface Sci.* **1994**, *166*, 109−117.
(16) Manica, R.; Connor, J. N.; Clasohm, L. Y.; Carnie, S. L.; Horn, R. G.; Chan, D. Y. C. *Langmuir* **2008**, *24*, 1381−1390.
(17) Rojas, C.; García-Sucre, M.; Urbina-Villalba, G. *Phys. Rev. E* **2010**, *82*, 056317−1−056317−15.
(18) Pushkarova, R. A.; Horn, R. G. *Langmuir* **2008**, *24*, 8726−8734.
(19) Nespolo, S. A.; Chan, D. Y. C.; Grieser, F.; Hartly, P. G.; Stevens, G. W. *Langmuir* **2003**, *19*, 2124−2133.
(20) Marinova, K. G.; Alargova, R. G.; Denkov, N. D.; Velev, O. D.; Petsev, D. N.; Ivanov, I. B.; Borwankar, R. P. *Langmuir* **1996**, *12*, 2045−2051.
(21) Franks, G. V.; Djerdjev, A. M.; Beattie, J. K. *Langmuir* **2005**, *21*, 8670−8674.
(22) McNamee, C. E.; Kappl, M.; Butt, H.-J.; Ally, J.; Shigenobu, H.; Iwafuji, Y.; Higashitani, K.; Graf, K. *Soft Matter* **2011**, *7*, 10182−10192.
(23) Barnes, G. T., Gentle, I. R. *Interfacial Science: An Introduction*; Oxford University Press: Oxford, 2005; p 86.
(24) McNamee, C. E.; Kappl, M.; Butt, H.-J.; Higashitani, K.; Graf, K. *Langmuir* **2010**, *26*, 14574−14581.
(25) McNamee, C. E.; Barnes, G. T.; Gentle, I. R.; Peng, J. B.; Steitz, R.; Probert, R. *J. Colloid Interface Sci.* **1998**, *207*, 258−263.
(26) Goddard, E. D.; Ackilli, J. A. *J. Colloid Sci.* **1963**, *18*, 585−595.
(27) Avila, L. V. N.; Saraiva, S. M.; Oliveira, J. F. *Colloid Surf., A* **1999**, *154*, 209−217.
(28) Jung, R. F., M.Sc. Thesis, The University of Melbourne, Melbourne, Australia, 1976.
(29) Tomoaia-Cotişel, M.; Zsako′, J.; Mocanu, A.; Lupea, M.; Chifu, E. *J. Colloid Interface Sci.* **1987**, *117*, 464−476.
(30) Robb, I. D. *Aust. J. Chem.* **1966**, *19*, 2281−2284.
(31) Deamer, D. W.; Meek, D. W.; Cornwell, D. G. *J. Lipid Res.* **1967**, *8*, 255−263.
(32) Gericke, A.; Hühnerfuss, H. *Thin Solid Films* **1994**, *245*, 74−82.
(33) Langmuir, I.; Schaefer, V. J. *J. Am. Chem. Soc.* **1937**, *59*, 2400−2414.
(34) Gaines, G. L., Jr. *Insoluble Monolayers at Liquid−Gas Interfaces*; Interscience: New York, 1966.
(35) Usui, S.; Healy, T. W. *J. Colloid Interface Sci.* **2001**, *240*, 127−132.
(36) Usui, S. *J. Colloid Interface Sci.* **1973**, *44*, 107.
(37) Usui, S.; Healy, T. W. *J. Colloid Interface Sci.* **2002**, *250*, 371−378.
(38) Wiese, G. R.; Janes, R. O.; Healy, T. W. *Disc. Faraday Soc.* **1971**, *52*, 302.
(39) Barhoumi, H.; Maaref, A.; Faffrezic-Renault, N. *Langmuir* **2010**, *26*, 7165−7173.
(40) Scheludko, A. D.; Nikolov, D. *Colloid Polym. Sci.* **1975**, *253*, 396−403.
(41) Preuss, M.; Butt, H.-J. *Int. J. Miner. Process.* **1999**, *56*, 99−115.
(42) Gillies, G.; Büscher, K.; Preuss, M.; Kappl, M.; Butt, H.-J.; Graf, K. *J. Phys.: Condens. Matter* **2005**, *17*, S445−S464.
(43) Exorewa, D.; Churaev, N. V.; Kolarov, T.; Esipova, N. E.; Panchev, N.; Zorin, Z. M. *Adv. Colloid Interface Sci.* **2003**, *104*, 1−24.
(44) Tagahashi, M. *J. Phys. Chem. B* **2005**, *109*, 21858.